Energy 127 (2017) 258–270

Contents lists available at ScienceDirect

Energy

journal homepage: www.elsevier.com/locate/energy

Methodology for estimating the ground heat absorption rate of Ground Heat Exchangers

Iosifina Iosif Stylianou [b, *], Georgios Florides [a], Savvas Tassou [b], Efthymios Tsiolakis [c], Paul Christodoulides [a]

[a] Faculty of Engineering and Technology, Cyprus University of Technology, Limassol, Cyprus
[b] Institute of Energy Futures, Brunel University London, Uxbridge, Middlesex, UB8 3PH, UK
[c] Geological Survey Department of the Ministry of Agriculture, Rural Development and Environment, Lefkosia, Cyprus

ARTICLE INFO

Article history:
Received 21 September 2016
Received in revised form
20 February 2017
Accepted 16 March 2017
Available online 29 March 2017

Keywords:
Geothermal energy
Ground Heat Exchangers
Low enthalpy systems
Ground geothermal properties
Heat load
GIS

ABSTRACT

In Ground Source Heat Pump systems, the heat exchange rate is an important factor with regard to the initial cost of the system. When the Ground Heat Exchanger (GHE) is installed in a lithology with high thermal properties in the presence of groundwater, the heat exchange rates are larger than in the cases with poor thermal response of the ground and no groundwater.

This research, hence, focuses on a methodology of measuring and analyzing the thermal properties of the lithologies encountered in an area, which can be used for the prediction of heat injection rates of a GHE, depending on its characteristics, the installation area ground properties and groundwater flow. A tool was created with the use of FlexPDE software, and a study case was chosen in order to validate the results. Twenty-two, 100 m in depth, boreholes located in Lefkosia (Cyprus) were tested through simulation for their geothermal performance over time. Subsequently the estimated heat load for the boreholes, after 24 h of operation in cooling mode, was used with the help of Geographic Information System software for the compilation of a heat load per meter depth map that can be transferred to the ground by a GHE. A review of similar studies and Geographical Information System applications referring to other countries is also presented and their results are compared to the results of this study. The step by step procedure presented in this paper can be used by engineers handling geothermal projects as a useful guide for sizing GHEs and calculating the heat injection rates of any area.

1. Introduction

Shallow geothermal energy is the heat stored beneath the surface of the earth and keeps the upper parts of the crust at a steady temperature, which is approximately equal to the mean annual atmospheric temperature of the year [12,25,27,35]. Technologies developed for the exploitation of this free energy type are getting more and more important as heating and cooling nowadays represent around 50% of EU's total energy consumption. Buildings consume more than 67% of thermal energy in Europe and has become a large untapped potential for renewable and energy efficiency [34].

Shallow geothermal energy constitutes a renewable energy source with high energy savings for heating and cooling in residential and commercial buildings. Ground Heat Exchanger (GHE) systems with the help of Heat Pumps can use the ground as a heat source or sink and achieve up to 70% energy savings compared to traditional heating/cooling systems [34]. In addition to their high efficiency, GHE systems are attractive due to their environmental friendliness.

In a Ground Source Heat Pump (GSHP) system during the heating cycle, a fluid circulates through the loop of the GHE absorbing heat from the ground, with the heat pump unit delivering heat into the building. For cooling, the process is simply reversed, with the GHE rejecting heat to the ground.

To design the GSHP system a thermal analysis is necessary. Its main objective is to predict the thermal response of the system and size the heat pump to be used. The efficiency of the geothermal project is greatly affected by the correct sizing of tubes [14], the tube configuration and the velocity of circulating liquid [8], the

* Corresponding author. 10, Megalou Alexandrou, 2682 Palaiometocho, Lefkosia, Cyprus.
E-mail address: Josephine.JS@live.com (I.I. Stylianou).

http://dx.doi.org/10.1016/j.energy.2017.03.070
0360-5442/

depth [28], the grouting material of the GHE [14,36,40], the existence of water flow in the underground layers [19,22] and the thermal properties of the earth [15,20,40].

The current paper discusses cases where it is desired to use GSHP systems to provide heating or cooling. Twenty-two study cases were set up to simulate the geothermal performance of boreholes over time, and to determine the heat injection load for these boreholes. Measurement and analysis of the thermal properties of the ground, the water level and velocity followed for obtaining actual design data. A validation tool was created with the use of FlexPDE software in order to achieve optimization of the system. The actual results and a series of maps drawn using the data can be used by engineers as a useful guide for sizing vertical GHE in their study (design) area, the Greater Lefkosia area. Similar maps can be compiled by engineers handling geothermal projects using the geological data of their area of interest and following the same methodology explained in Sections 3 and 4.

Similar studies, concerning the simulation of the performance of vertical GHE over time and the determination of the thermal load and amount of energy extraction that can be sustained are also available for Germany, Japan, England, Wales, France and Ireland and are presented in the following studies.

Ref. [9] determined and assessed the economic and technical factors that influence the design and performance of GSHP systems in southern Germany in private households. Moreover, the spatial correlation of these design and performance factors with the geology, legislation, population issues, and climatic conditions using real data was evaluated. This theoretical study is based on large-scale systems, i.e. system capacity $\geq$175 kW and the determined specific heat extractions used a range between 33 and 63 W m^{-1}. Although spatial variations of the specific heat extractions are locally observed, the majority of the studied zones have average specific heat extractions between 48 and 50 W m^{-1} showing no or only a minor correlation between the chosen specific heat extraction and the site-specific geology.

For Japan two studies, one for Chikushi Plain and a second one for the capital city, Tokyo, are presented [30]. Estimated the effect of the ground's thermal properties on a GHE system performance using a numerical simulation tool in the 23 wards of Tokyo. A method to develop the energy potential for GSHP systems was suggested and its application was performed using geographical information system (GIS) data. Their results showed that the heat exchange rates in cooling season have a very small variation, from 40 to 42 W m^{-1}.

Ref. [21]; in their study developed suitability maps for the installation of GSHP systems for the Chikushi Plain, western Japan. The maps were created through a combination of groundwater field-survey data and numerical modeling of the groundwater flow system. Single GHE models were then constructed to simulate the heat exchange performance at different locations in the plain and the results were used for the creation of the suitability maps for GSHP systems. The authors came to the conclusion that variations in the heat exchange rates of over 40% revealed by the map were ascribed to differences in the GHE locations, confirming how important is to use appropriate thermophysical data when designing GSHP systems.

Studies concerning the simulation of the thermal load and amount of energy extraction that can be sustained in a GSHP systems for England and Wales were done by Refs. [3,4] and [2]. In more detail, a web-based screening tool was developed by the British Geological Survey (BGS) (see http://mapapps2.bgs.ac.uk/gshpnational/home.html) and highlights areas where conditions may be suitable for installing commercial-scale (>100 kW heating or cooling demand) open-loop GSHP systems [2,3,4]. Areas are considered 'favorable' when one (or more) productive bedrock aquifer (i.e. with yields of at least 1 L s^{-1}) is present within 300 m beneath the ground (topographic) surface. The performance of the screening tool was tested by applying the tool to locations where commercial-scale GSHP systems are known to be operational. The study estimated that about 56% of the area is suitable for open-loop installations with a capacity of 100 kW or more. The UK Government expects that, by 2020, 12% of the UK's heat demand will come from renewable sources, and this tool is providing incentives to help achieve this scope.

In France, the French geological survey, BRGM (*Bureau de Recherches Géologiques et Minières*) became a pioneer in the area of GSHP usage in 2005, with the production of an atlas of geothermal resources in near-surface aquifers in the Paris region [7]. The value of such atlases was confirmed by the Grenelle environment consultations, which set a heat production goal of 550 ktoe (kilotonnes oil equivalent) for very low energy geothermal power by 2020 (up from 40 ktoe in 2006). The purpose of these kind of atlases was to identify geothermal resources in near-surface aquifers (0–100 m below the surface, sometimes 0–200 m) that are likely to be of interest for deploying geothermal energy production via heat pumps for heating, domestic hot water and cooling. Using a 500 $\times$ 500 m grid, the atlases describe the geothermal resources of near-surface aquifers via a multi-criteria analysis combining productivity, water temperature and access depth, and sometimes water chemistry if it is likely to be incompatible with geothermal applications. BRGM offers free online access at www.geothermie-perspectives.fr. Note that maps present no heat exchange values, but just an indication for favorable and less favorable areas for GSHP systems installations.

In Ireland, a homeowner manual was published in 2015 for GHE usage [10]. The aim of that publication was to help readers with the decision to purchase and install a domestic GSHP system for home heating. In the manual information on subsoil, bedrock and aquifers can be found through a series of maps: Groundwater resource or Aquifer map, Groundwater vulnerability map, Subsoil type map, Subsoil permeability map and Ground source heat suitability maps. Suitability maps concern vertical and horizontal closed-loop systems and open-loop Domestic and commercial suitability map. Maps again give only an indication if the area is classified as highly suitable, suitable, possibly suitable or generally unsuitable without specifying any heat exchange rate. In addition, maps can be queried interactively via the GSI's webmapping at http://www.gsi.ie/Mapping.htm.

In addition, there exist many other studies presenting only underground thermal conductivity maps in order to classify an area as suitable or not for vertical GHE installation. Refs. [37,29] presented the Thermal Conductivity Maps of Calabria (Italy) and Oslo (Norway) respectively. Additionally [16], presented a study for Trentino area, Italy, while [17] presented the ThermoMap project and a series of thermal conductivity and heat capacity maps of Constanta (Romania).

The methodology used in our research is explained in the sections that follow. In Section 2 is presented the geological structure of the Greater Lefkosia Area that was used as a study case. In Section 3 the geological sampling is carried out and the thermal properties of different lithologies of Greater Lefkosia are measured in the laboratory. Based on the data of the collected samples thermal conductivity λ and specific heat capacity *cp*, maps of the study area are drawn with the use of the Geographical Information System (GIS). In Section 4 twenty-two study cases are set up and the influence of the ground on the GHE output is investigated numerically. The results are used for the compilation of the "Design Load Map of Ground Heat Exchangers for the Greater Lefkosia Area". We conclude with Section 5 where our main findings and observations are compared with other similar projects, as well as with Section 6

where the implications of our study are further discussed.

2. 3D Geological Modeling of the study area

Lefkosia (Nicosia) is the capital city of Cyprus with the highest density of population on the island and with 19.5% increase in population from 2001 to 2011 [13]. Geographically it is located in the center of the island in the Mesaoria Plain, which is topographically low, a rather flat area between the Troodos Range to the south-east and the Pentadaktylos Range to the north. The climate is Mediterranean, with long, warm, dry summers from June to October and mild winters with occasional rain, lasting from December to April. The following temperatures were recorded by the Meteorological Service of the Republic of Cyprus, in 2010, near Lefkosia city: during winter from 0 °C (nighttime) to 24 °C (daytime) and during summer from 18 °C (nighttime) to 45 °C (daytime). Under these climate conditions GHEs can be widely used together with geothermal heat pumps in Lefkosia with high potential of energy savings for heating and especially for cooling. For these reasons the Greater Lefkosia Area was chosen for this study.

From the geological point of view, the study area is extensively analyzed by the "Bedrock Geologic Map of the Greater Lefkosia Area" [26]. "Geologic" or "geological" map is a general term used by geologists to describe the rock types, usually solid, that underlie the soils or other unconsolidated, superficial material [31]. More simply, it shows the lithified rocks that lie under the loose softer material at the surface of the Earth, up to an unspecified depth.

The island is divided into four geological terranes, the Kyrenia or Pentadhactylos Range, the Troodos Ophiolite Complex (Range), the Mamonia Complex and the Circum Troodos Sedimentary Succession (or Mesaoria Plain) [23,32,43] as shown in Fig. 1. Each terrane is the product of different tectonically deposition and the area of Lefkosia map is divided between the Kyrenia terrane and the circum Troodos sedimentary succession. The area covered by the present study is also shown on the regional map of Fig. 1. Further on, Ophiolitic rocks of the Troodos are shown to lie in the subsurface of Lefkosia area and the Ovgos fault zone is the boundary between (a) the Kyrenia terrane and the Circum Troodos Sedimentary Succession and (b) the Kyrenia and Troodos terranes in depth [26].

For the needs of our research a 3D geological model was created (Fig. 2), in order to visualize the study area, examine its thermal response and the potential of vertical GHE usage in the area. For the design of the 3D model, geological data derived from the project "Seismic Hazard and Risk Assessment of the Greater Nicosia Area" were used. The program was established in 1998 with funds provided mainly by the United States Agency for International Development (USAID) and also by the United Nations Development Program (UNDP) and ended in 2004. "Bedrock Geologic Map of the Greater Lefkosia Area" [26] was also compiled in the framework of that project. The geological mapping was based on fieldwork mapping, geological age dates, several deep boreholes and an interpretation of a seismic-reflection dip log by the Forest Oil Company. The Lakatameia area was penetrated by the exploration hole KL–1, which was drilled by the Forest Oil Company in the 1960s. This borehole, which reached a depth of 2400 m, is shown on the cross section of the geological model (Fig. 2).

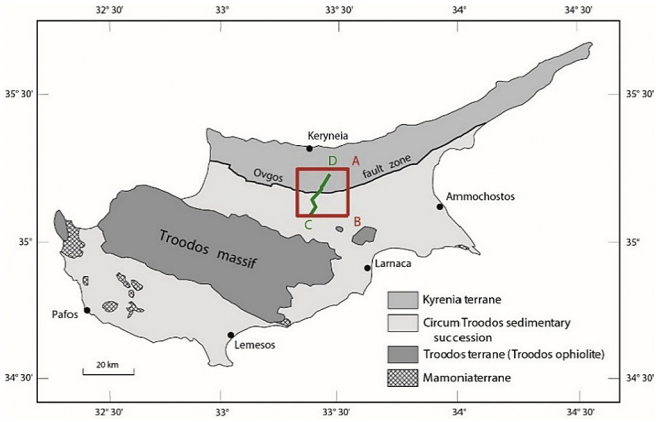

Fig. 1. Map of the four major tectonic-stratigraphic terranes of Cyprus [26] and the [23]. The red box shows the boundary of the Lefkosia geologic map. The green line (CD) is the cross section line shown in Fig. 2. (For interpretation of the references to colour in this figure legend, the reader is referred to the web version of this article.)

The 3D model was designed based on "Bedrock Geologic Map of the Greater Lefkosia Area" [26] with the use of the ArcGIS and Adobe Illustrator software. In more detail, ESRI ArcGIS package of software which provides the ability to visualize geological data in 3D was used, for creating the surface of the model. Then, using Adobe Illustrator graphic software, the cross section was "attached" to the 3D geological surface already created in ArcGIS.

On the 3D model 9 different geological formations are found as shown below:

a) Apalos Formation (Pleistocene) - Gravel, sand, silt and clay.
b) Nicosia Formation (Pliocene and Lower Pleistocene) - Undivided formation shown on cross section only (members are explained below).
c) Kalavasos Formation (Late Miocene, Messinian) - Gypsum, anhydrite, chalky marl and marly chalk; most commonly occurs as massive gypsum.
d) Lapatza Formation - Siltstone, marl, chalky marl, marly chalk and limestone.
e) Kythrea Formation - Greywacke, marl, sandstone and siltstone; dominantly flysch.
f) Pakhna Formation (Early, Middle, and Late Miocene) - Predominantly chalk with lesser chalky marl and marly chalk.
g) Lefkara Formation (Palaeogene and Cretaceous) - Shown on cross section only, chalk, marl, marly chalk, chalky marl with in places bands or nodules of chert.
h) Moni Formation (Cretaceous) - Shown on cross section only, melange of older (Triassic - Cretaceous) blocks of yellow quartz sandstone, grey siltstone, serpentinite and other lithologies entrained in a matrix of silt and bentonitic clay.
i) Troodos Ophiolite Complex (Cretaceous) - Shown on cross section only, mafic and ultramafic ophiolitic rocks.

In addition to the above, Nicosia Formation is divided into seven geological members:

1. The Marine Littoral Member - Gravel, sand and silt deposited in an intertidal zone.
2. The Aspropamboulos Oolite Member - Fine-grained oolite. Unidirectional, planar cross beds directed to the south.
3. The Lithic Sand Member - Dominantly lithic sand, but also includes lesser marl, silty marl and calcarenite.
4. The Athalassa Member - Calcarenite and bioclastic calcarenite.
5. The Kephales Member - Marine gravel, cobbles, pebbles, and sand. Clasts are dominantly derived from the Troodos Ophiolite and lesser from Tertiary carbonate deposits.
6. The Marl Member - Marl, silty marl, and lesser sandy marl. Fossilliferous and typically khaki-green in color; weathered surfaces are yellow-brown in color.
7. The Basal Conglomerate Member - Gravel, cobbles, coarse sand. Clasts are dominantly derived from the Troodos Ophiolite Complex.

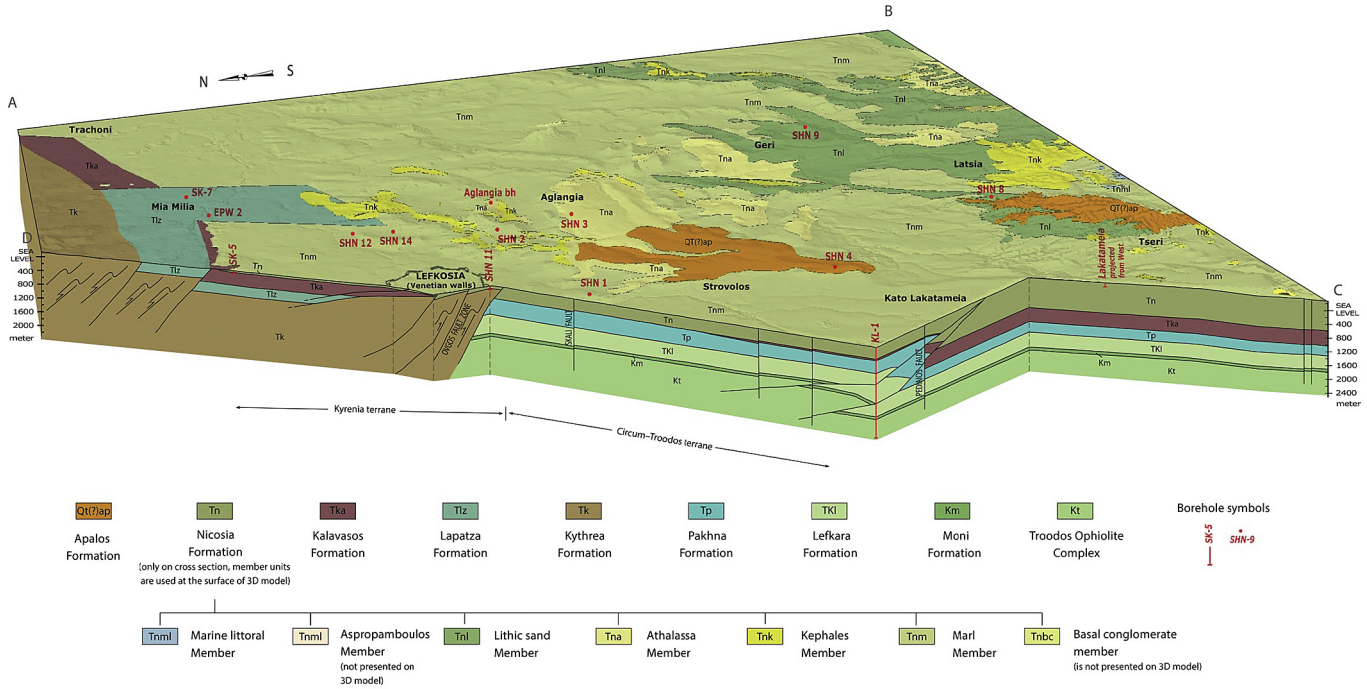

Fig. 2. 3D Geological Model based on data of the "Bedrock Geologic Map of the Greater Lefkosia Area" [26].

3. Thermal properties of Lefkosia bedrock

In order to proceed with any geothermal project concerning the geothermal performance of GHEs, the thermal properties of the geological units presented in the study area must be defined. In our study case the "Bedrock Geologic Map of the Greater Lefkosia Area" [26] was used and the geothermal response was estimated as follows.

3.1. Geological sampling

Due to the difficulty of measuring thermal properties in situ, a geological sampling was performed in the study area and measurements took place in a laboratory. Apalos, Nicosia, Kalavasos, Lapatza and Kythrea were the geological formations included in this study. In more detail, Nicosia Formation consists of the Aspropamboulos Oolite Member, Lithic Sand Member, Athalassa Member, Kephales Member and the Marl Member. The Basal Conglomerate Member and the Marine Littoral Member of the Nicosia Formation are very small units on the map and were not included in this study. In addition, Marine Member layers do not exceed thicknesses of more than 10 m in any area and Basal Conglomerate can be found only in very small areas within the Ovgos fault zone having no geothermal significance. Samples were collected from the surface, except in some cases for the north part of the study area, were samples were obtained from the archive of the Cyprus Geological Survey Department.

3.2. Thermal testing

The thermal properties of 26 geological samples were obtained in laboratory at room temperature using the apparatus ISOMET 2104 Heat Transfer Analyzer. More precisely, thermal conductivity λ, thermal diffusivity α and volumetric heat capacity V (density multiplied by specific heat capacity) were measured after the samples were dried in an oven at 110 ± 10 °C for 24 h (ASTM-C-332).

ISOMET 2104 is a portable commercial apparatus for direct measurement of heat transfer properties. The measurement process is based on the analysis of a temperature response of the analyzed material to heat flow impulses. The heat flow is induced in a resistor of the probe by a distributed electric power (ASTM-D-5334-08 and ASTM-D-5930-09). The user manual of this device (Applied Precision -ISOMET) gives the accuracy of the thermal conductivity to be 5% of the reading + 0.001 W m^{-1} K^{-1}. In the case of the volumetric heat capacity the accuracy is 15% of the reading 1 J m^{-3} K^{-1}. The apparatus is equipped with two types of measurement probes: needle probes for soft materials, and surface probes for hard materials.

For conducting measurements with the surface probe of the Isomet 2104 Heat Transfer Analyzer a smooth flat surface was required. In order to create the flat testing surface, a rock cutting machine and a polishing machine were used. At least two flat testing surfaces with a minimum size of 7 × 7 cm^2 were created. The minimum thickness to enable the test was 2.5 cm.

In order to calculate the specific heat capacity *cp* of the samples, their density ρ was also measured in the laboratory (specific heat capacity = volumetric heat capacity/density). Because most of our samples were of irregular size, densities of the collected samples were defined by laboratory tests based on CYS-EN-13383-2:2011. In cases of small in size or soluble in water samples, volumes were measured using the *Displacement Method* (*Archimedes Principle*).

3.3. Laboratory results

Laboratory tests for measuring the thermal properties of the collected geological samples were repeated two or three times on each sample. Mean values were calculated based on the geological type of the tested samples (Table 1).

Totally 16 samples were collected from the Nicosia Formation, 3 from the Lapatza Formation, 3 from the Kythrea Group (excluding Lapatza Formation), 3 from the Apalos Formation and 1 from the

Table 1
Mean values of measured thermal conductivity λ, thermal diffusivity α, density ρ and calculated specific heat capacity c_p per geological unit.

Geological unit (abbreviation)		Thermal diffusivity $\times 10^{-6}$ (m^2s^{-1})	Thermal conductivity (W m^{-1} K^{-1})	Calculated specific heat Capacity $\times 10^{-3}$ (J K^{-1} kg^{-1})	No of samples tested
Apalos formation (QT(?)ap)		0.42	0.60	0.85	3
Nicosia formation (Tn)	Aspropamboulos Oolite Member (Tnas)	0.41	0.62	0.93	2
	Lithic Sand Member (Tnl)	0.49	0.73	1.02	1
	Athalassa Member (Tnas)	0.64	0.89	0.79	9
	Kephales Member (Tnk)	0.93	1.48	0.60	2
	Marl Member (Tnm)	0.39	0.56	0.76	2
Kalavasos formation (Tka)		0.65	1.02	0.63	1
Lapatza formation of the Kythrea Group (Tlz)		0.95	1.42	0.65	3
Kythrea group exluding Lapatza Formation (Tk)		0.51	0.73	0.76	3

Kalavasos Formation.

Care was taken in the collection of samples to represent the geology at the corresponding depth in the boreholes. For this reason, surface samples were excluded. Instead samples were collected from nearby road cuts, cliff or sloping sides to make sure that collected samples went the same geological processes as the corresponding borehole strata.

Table 1 shows that the mean values of the thermal conductivity of all the samples are between 0.56 and 1.48 W m^{-1} K^{-1}. Calculated values for specific heat capacity are also in a very small range from 0.60 to 1.02 $\times$ 10^{-3} J K^{-1} kg^{-1}.

Results are further analyzed in Figs. 3 and 4, where one can see that each geological formation presents a range of values for each thermal property. This is due to the variety of lithologies that are present in each geological formation (see Section 2) and the specific properties of the samples measured. Sample properties like grain size, amount and type of impurities, geological compression when the sample was formed and many others affect greatly the thermal properties of the sample.

3.4. Thermal Conductivity and Specific Heat Capacity maps of the Greater Lefkosia Area

Thermal Conductivity and Specific Heat Capacity maps (Figs. 5 and 6) were created with the use of the Geographical Information System (GIS). In this research the ArcGIS package of software (ESRI) was used in order to compile the maps. With the help of the software, each bedrock geological unit presented on the "Bedrock Geologic Map of the Greater Lefkosia Area" [26] was assigned the mean value of the corresponding tested samples (Table 1).

The Thermal Conductivity Map in Fig. 5 shows low values for the biggest part of the map and only a small part of the study area has values above the average. On the other hand, the Specific Heat Capacity Map (Fig. 6) shows the biggest part of the study area with an average value of 0.6 $\times$ 10^{-3}JK^{-1} kg^{-1}. In both cases this is due to the fact that a large part the Bedrock Map is covered with Marl Member of the Nicosia Formation which has poor thermal response.

All the above values were taken in the laboratory under constant pressure. Although pressure may be a key parameter that affects the final thermal performance of geological samples [[1,24,42]], the effect of pressure on thermal conductivity is small at pressures below 100 MPa (1000 bar) - [1,41]. In more detail [1] presents the results of thermal conductivity measurements for dry porous rock sandstone (porosity of 13%). Pressure dependence up to 100 MPa did not exit the 8% of the value measured under atmospheric pressure. In addition [41], presents measured values for Pyrex Glass, Basalt, Limestone, Teflon, Halite and Quartz. Values presented only 3% increased at 100 MPa.

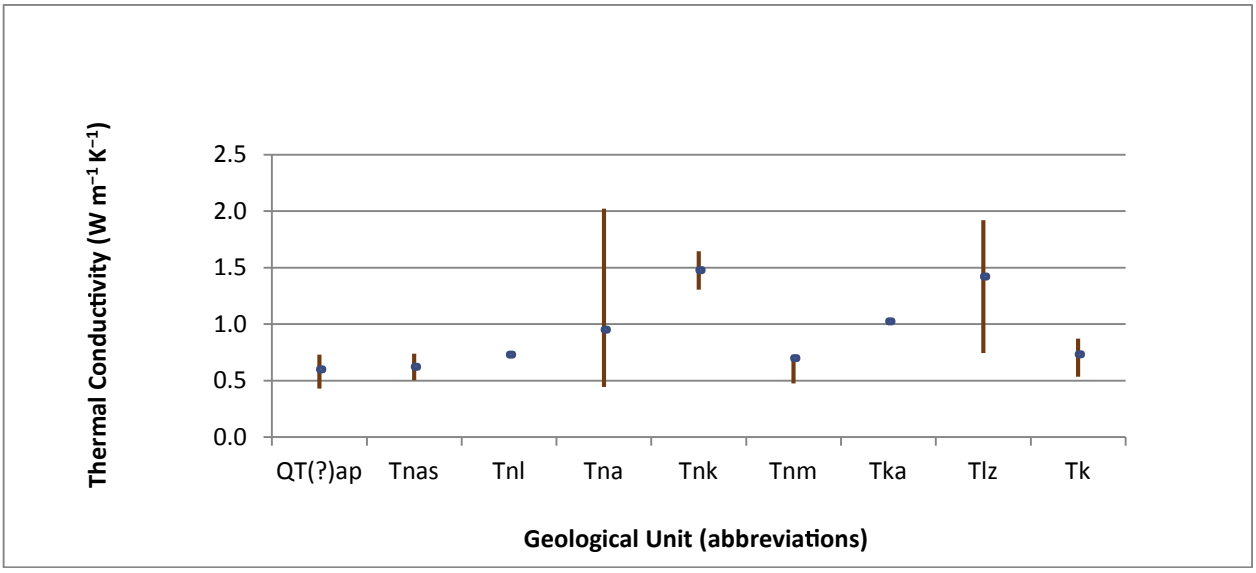

Fig 3. Range of values measured in the laboratory for thermal conductivity λ grouped by the geological formation/member of sample (the mean value is presented with a dot in blue color). (For interpretation of the references to colour in this figure legend, the reader is referred to the web version of this article.)

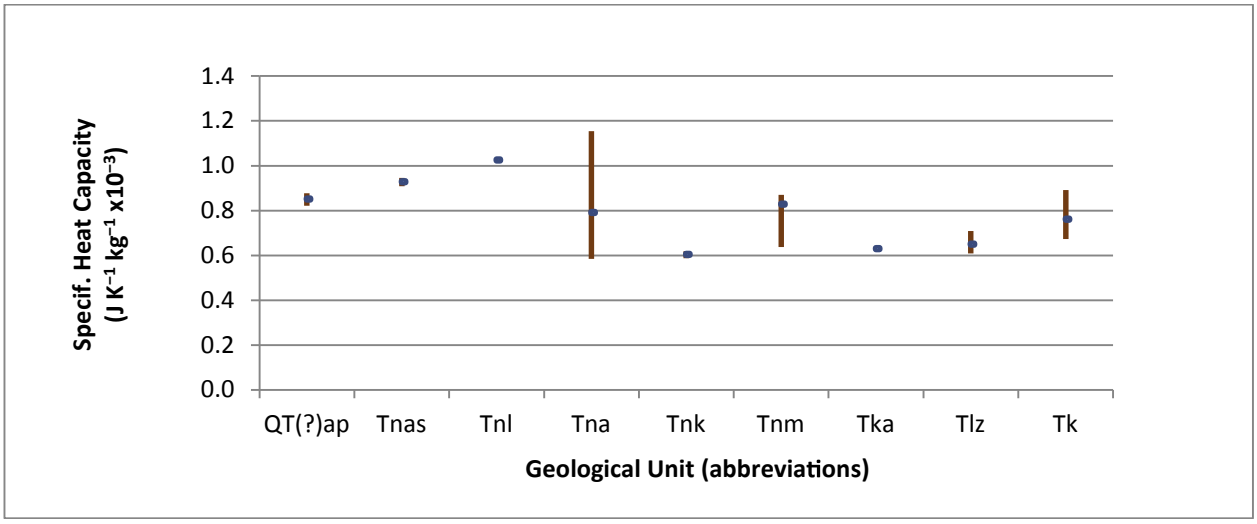

Fig 4. Range of values measured in the laboratory for specific heat capacity c_p grouped by the geological formation/member of sample (the mean value is presented with a dot in blue color). (For interpretation of the references to colour in this figure legend, the reader is referred to the web version of this article.)

4. Ground Heat Exchanger usage in the Greater Lefkosia area

As already said, the main objective of this research is to provide engineers with a method to be followed for sizing vertical GHEs in a study area. This will be achieved through setting up a large number of representative study cases covering the extent of the area of interest. In our example 22 representative study cases were chosen in different geological and geographical locations, as can be seen in Fig. 7 (some of them appear in Fig. 2 as well). In each case the influence of ground on the performance of the GHE was investigated so as to calculate the heat load per meter depth that can be transferred to the ground in each borehole of the studied area.

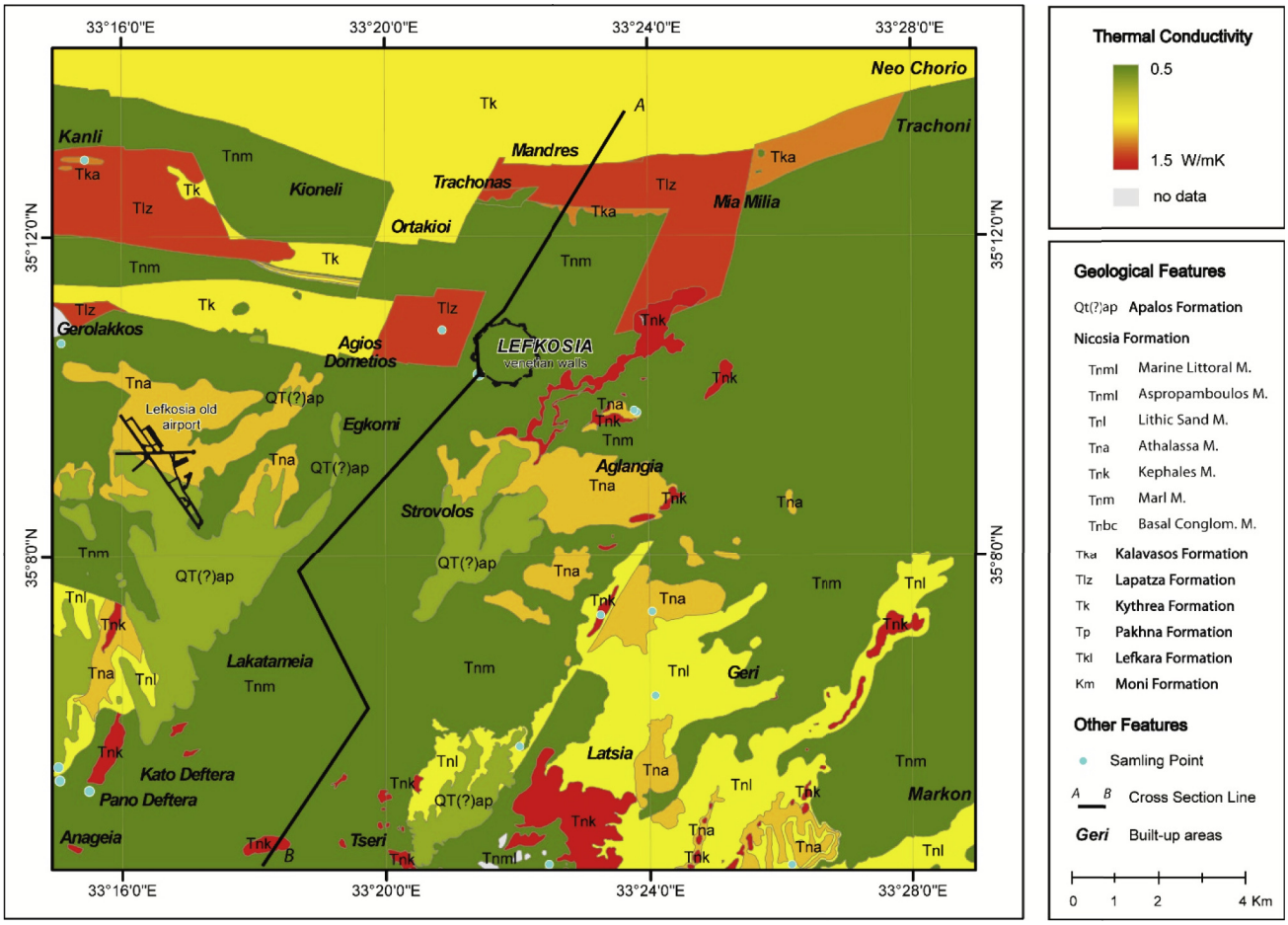

Fig 5. Thermal conductivity map of the Greater Lefkosia area.

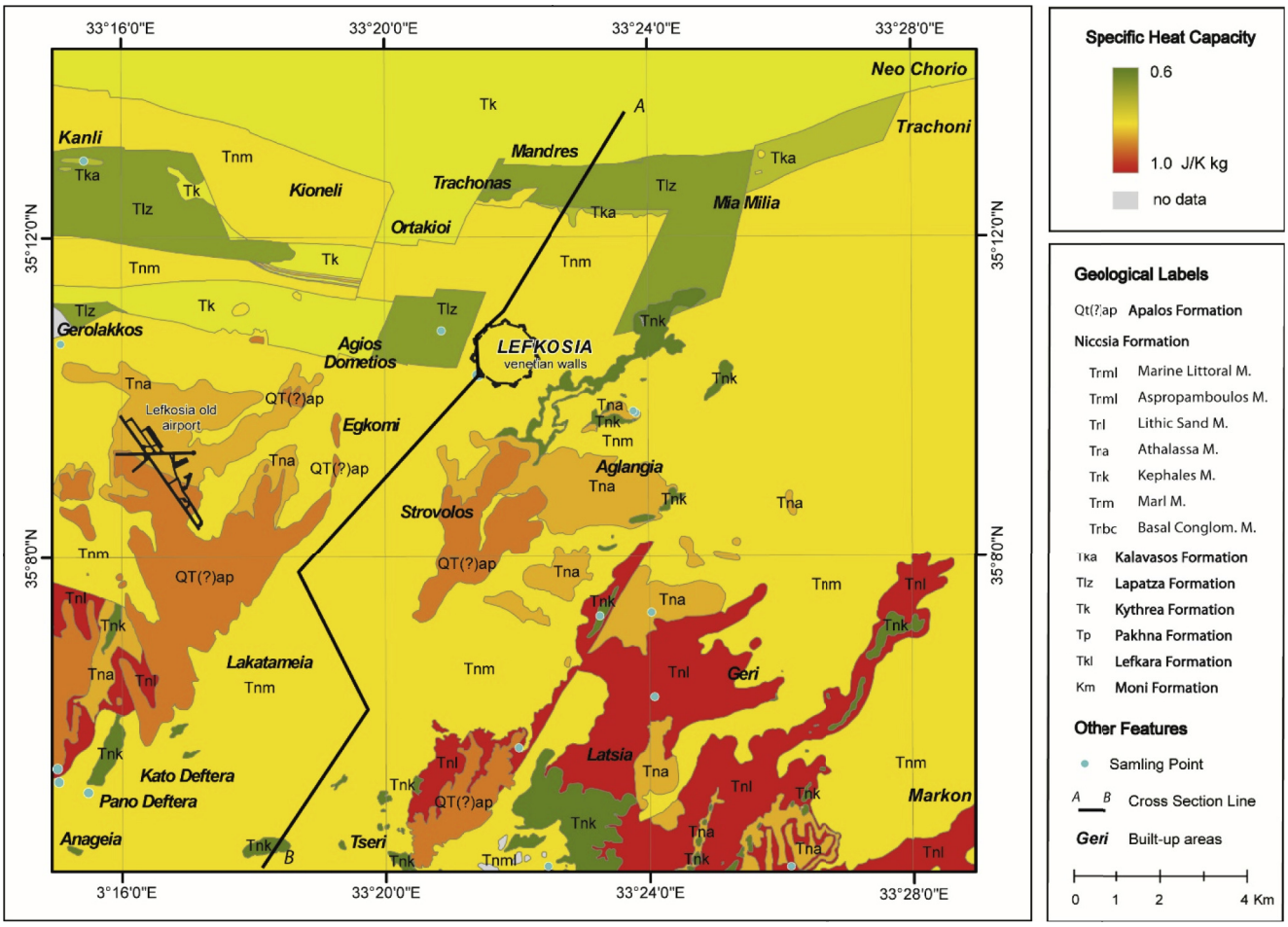

Fig. 6. Specific heat capacity map of the Greater Lefkosia area.

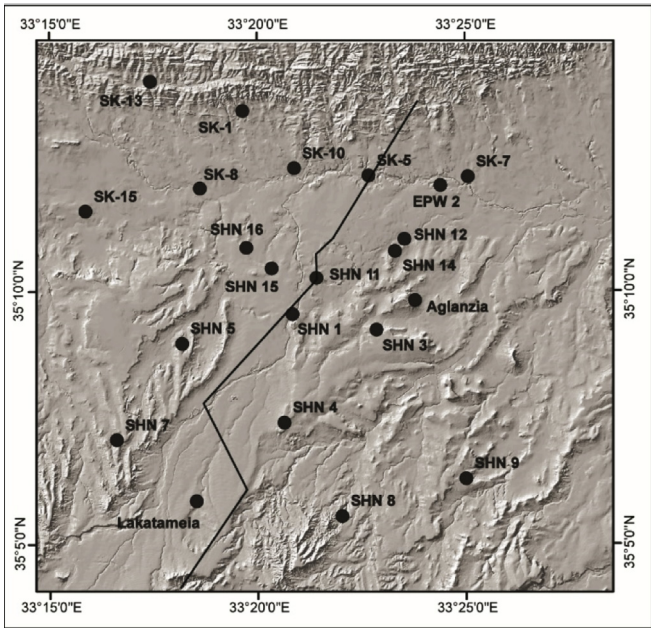

Fig 7. Location map of boreholes used as study cases (the digital elevation model used as background was provided by the Cyprus Geological Survey Department).

4.1. Mathematical model

The performance of the GHEs was calculated using a validated model in FlexPDE software. The results are tabulated in Table 3 and can be used as a guide for engineers designing GHEs in the Greater Lefkosia Area.

The FlexPDE software was chosen as the numerical solving tool, because it is a script-driven program that can combine parameters – i.e. equations and boundary conditions – entered by the user and obtain numerical solutions of 3D differential equations, based on the Finite Element Method [5]. For the cases under study, heat distribution over time is described by the general heat transfer equation based on the energy balance. The rate of energy accumulated in the system is equal to the flow of energy entering the system, plus the rate of energy generated within the system, minus the flow of energy leaving the system.

The 3D conservation of the transient heat equation is used and applied in FlexPDE software:

$$\rho c_p \frac{\partial T}{\partial t} + \rho_w c_{pw} u \nabla T + \nabla \cdot \mathbf{q} = Q \quad (1)$$

where T is the temperature, t is time, ρ is the density of the borehole/surrounding soil and rock material, c_p is the heat capacity of the borehole/surrounding soil and rock material at constant pressure, ρ_w is the density of the heat transferred fluid, c_{pw} is the heat capacity of the heat transferred fluid at constant pressure u is the

velocity of the groundwater, Q is the heat source and $\mathbf{q}$ is Fourier's law heat conduction that describes the relationship between the heat flux vector field and the temperature gradient:

$$\mathbf{q} = -\lambda \nabla T \tag{2}$$

where λ is the thermal conductivity of the borehole/soil/rock material.

In Eq. (1) the first term represents the difference in internal energy, the second term is the part of the heat carried away by the flow of water, the third term represents the net heat conducted as described in Eq. (2) and the fourth is the heat source.Where groundwater is present in the underground layers, the heat transfer Eq. (1) [6] becomes:

$$\rho_{eff} c_{p.eff} \frac{\partial T}{\partial t} + \rho_w c_{pw} u \nabla T + \nabla \cdot \mathbf{q} = Q \tag{3}$$

where $\rho_{eff} c_{p.eff}$ is the effective density and volumetric heat capacity of the porous media at constant pressure, given by:

$$\rho_{eff} c_{p.eff} = \theta_s \rho_s c_{\rho s} + (1 - \theta_s) \rho_w c_{pw} \tag{4}$$

where θ_s is the soil material volume fraction given in a percentage from 0 to 1, ρ_s is the density of the porosity solid material, $c_{\rho s}$ is the volumetric heat capacity of the porosity soil material, and $\rho_w c_{pw}$ are the density and the volumetric heat capacity of the heat carrier fluid. The velocity u in the second term of Eq. (1) represents Darcy's velocity (see next section).

The heat conduction in Eq. (3) $\mathbf{q}$ can be expressed as:

$$\mathbf{q} = -\lambda_{eff} \nabla T \tag{5}$$

where λ_{eff} is the effective thermal conductivity.

In our case a weighted geometric mean of the thermal conductivity of both the solid and the fluid materials is needed, and is given by:

$$\lambda_{eff} = \lambda_s^{\theta_s} \lambda_w^{(1-\theta_s)} \tag{6}$$

Note that the numerical model, as described above, has been validated by Ref. [20].

4.2. Ground Heat Exchanger design – applications in real boreholes

The thermal contact of (a) the borehole wall, (b) the tubes and (c) heat transferred fluid inside the tubes are controlled by the following factors: tube material, thickness of tube wall, tube size and configuration, space of tubes, properties of the fluid inside the tubes, flow rate of the fluid, borehole diameter and annular space filling [38].

In our study cases we refer to a geothermal system combining a borehole heat exchanger and the surrounding soil mass crossed by an aquifer. A vertical GHE was set up in each borehole consisting of a descending and an ascending leg of polyethylene pipe connected at their ends with a U-joint. Boreholes (BHs) have a diameter of 0.2 m and were filled with thermally enhanced bentonitic clay [18]. Bentonitic clay has the ability to expand and completely fill the borehole and hold firmly the GHE in place. Water was used as the heat carrier fluid, circulating in the tubes. In the analysis the area considered was equal to 0.5 m around the borehole and a depth of 100 m was assumed. The tubes used are of 100 m length, 0.0285 m inner diameter and 3.5 mm wall thickness. The distance between the center of the tube and the center of borehole is 0.048 m. The initial temperature of the ground is set to 22 °C for the entire study area (based on temperatures measured inside Lakatameia BH) and the temperature of circulating water at 40 °C in order to satisfy the requirements of the heat pump. The heat pump type was chosen in accordance to the results of the Technical Requirements Checklist (TRC) test that took place again at Lakatameia BH. Geothermal borehole basic parameters as used in the simulations are presented in Table 2.

Table 2
Operational parameters used in simulation.

Property	Value	Unit
Fluid velocity in tubes	0.32	m s^{-1}
Fluid initial temperature in tubes	40.0	°C
Wall thickness of heat exchanger tube	0.0035	m
Distance between center of borehole to center of each heat exchanger tube	0.048	m
Temperature of ground	22	°C
Borehole radius	0.1	m
Length of heat exchanger	100	m

The knowledge of the geological and hydrological (water level) conditions were necessary for the correct parameter setting. Fig. 8 shows the geological log data for each borehole based on the actual geological data arising from the Seismic Hazard and Risk Assessment Project of the Greater Nicosia Area. Lakatameia BH was part of a project undertaken by the Cyprus University of Technology (finished in 2011) for the efficient use of Ground Coupled Heat Pumps in Cyprus. In that project the underground temperatures were recorded throughout the year. Recorded undisturbed temperatures in Lakatameia BH stayed constant at 22 °C for depths between 7.5 and 100 m throughout the year [33].

Geological changes for the surface layer (up to 7 m depth) were not taken into consideration, as some boreholes (SHN 1, SHN 2, SHN 16, etc.) were very close to rivers and Alluvial Deposits were found on top. In some other cases (SHN11, SHN 12, etc.) manmade materials were found on the surface layer. In addition, surface layer is affected from seasonal ambient temperature and water flow resulting from rainfall, factors which were neglected in this research.

Water level in each borehole was also considered in calculations, as the flow of underground water may have an important effect on cooling of the vertical heat columns of the heat exchangers. At the north part of the study area actual data were not available and water levels were estimated from other boreholes near the study cases. Simulations were also based on observations of the Geological Survey Department of Cyprus concerning the groundwater velocity; values used in the simulations are from 20 up to 30×10^{-7} m s^{-1}. The only exception is the Marl lithology where the underground water velocity used in the calculations was only 0.1×10^{-7} m s^{-1}.

4.3. Results

In this section the output results of FlexPDE software are presented. Fig. 9 shows the results for the heat load transferred to the earth through the GHE, as calculated by FlexPDE software for each study case. Results are calculated based on the temperature difference of circulating water as represented by the equation:

$$Q = m c_w \left(T_f - T_i \right) \tag{7}$$

where Q is the amount of heat energy lost by the circulating water in the tubes, m the mass of water that was circulated, c_w the specific heat capacity of water, T_f the final (output) temperature of circulating water and T_i the initial (input, entering) temperature of circulating water.

Table 3
GHE heat loss per meter (W m^{-1}) after 12, 18 and 24 working hours.

Borehole	Heat load per meter (W m^{-1})		
	after 12 h	after 18 h	after 24 h
SHN 7	46	44	42
SHN 15	42	39	38
SHN 1, SHN 5, SHN 11, SHN 12, SHN 14, SK-1, SK-7, SK-8, SK-10, SK-13, SK-15, EPW 2, Aglanzia BH	40	37	36
SHN 3, Lakatameia BH	38	36	34
SK-5, SHN 9	37	35	34
SHN 8	33	31	30
SHN 16	40	33	29
SHN 4	30	28	26

In Fig. 9 GHEs heat load values are monitored for the first 24 working hours. Values decrease with time, as the difference between input and output temperature of circulating water also decreases. Note that SHN1, SHN12, SHN14 and Aglatzia BH, although they have the same lithology with Lakatameia BH, they exhibit different heat loads. Heat load changes are proportional to the changes of water level in these cases. In the cases where heat exchanger surrounding material and water level in the borehole are the same, density is the key factor for the prediction of the thermal response of the borehole. For example, from our study cases, SHN1, SHN12 and SHN14 have the same lithology and almost the same water level with SHN15, but the heat exchanger surrounding material (despite the same lithology for all cases) have higher density values at the area where SHN15 is located. Heat loss results for each study case are analytically presented in Table 3 after 12, 18 and 24 h of continuous operation.

It turns out that SK-5 exhibits a much lower heat loss value compared to all other boreholes located at the north part of the study area (see Fig. 7). This is due to the Gypsum lithology that is present at the drilling location. Gypsum has a unique thermal response compared to other lithologies, as it exhibits higher thermal response under dry conditions than under water saturated conditions [39].

4.4. Suitability map of GHEs for the Greater Lefkosia Area

The heat loss data used in generating the "Design Load Map of Ground Heat Exchangers for the Greater Lefkosia Area" (Fig. 10) resulted from calculations as explained above. Calculated data for the 22 study cases and for GHE operating for 24 h (Table 3), were interpolated with ArcGIS software using the Kriging method. This method was chosen as it is an interpolation method based on a statistical model that includes autocorrelation. Because of this, Kriging geostatistical technique not only has the capability of producing a prediction surface but also provides some measure of the certainty or accuracy of the predictions. The digital elevation model presented on the background of the map (Fig. 10) was also created with the use of ArcGIS software supplied by licence of the Cyprus Geological Survey Department.

The values that resulted from interpolation and are presented on the map, vary between 26 and 42 W m^{-1}. It is important to note that the heat loss data used for interpolation are not evenly distributed throughout the map. Small areas with dense data surrounded by wide areas containing sparse data are characteristic of the heat load map. As such, the user should keep in mind that the heat loss map is well constrained in areas of dense data and more interpretive in areas of sparse data.

Fig. 10 can be used as a tool for visualizing and easily understanding the potential of GHE usage in the Greater Lefkosia Area. From the map it can be visualized that, generally, the heat load transferred to the earth through the GHEs at the north part of the study area is much higher than the transferred heat load at the southern areas. This is due to (a) water levels that are higher at the north part, and (b) the fact that different geological formations are present in the two areas, as they are part of different geological terranes (see Section 2, "3D Geological Modeling of the Study Area").

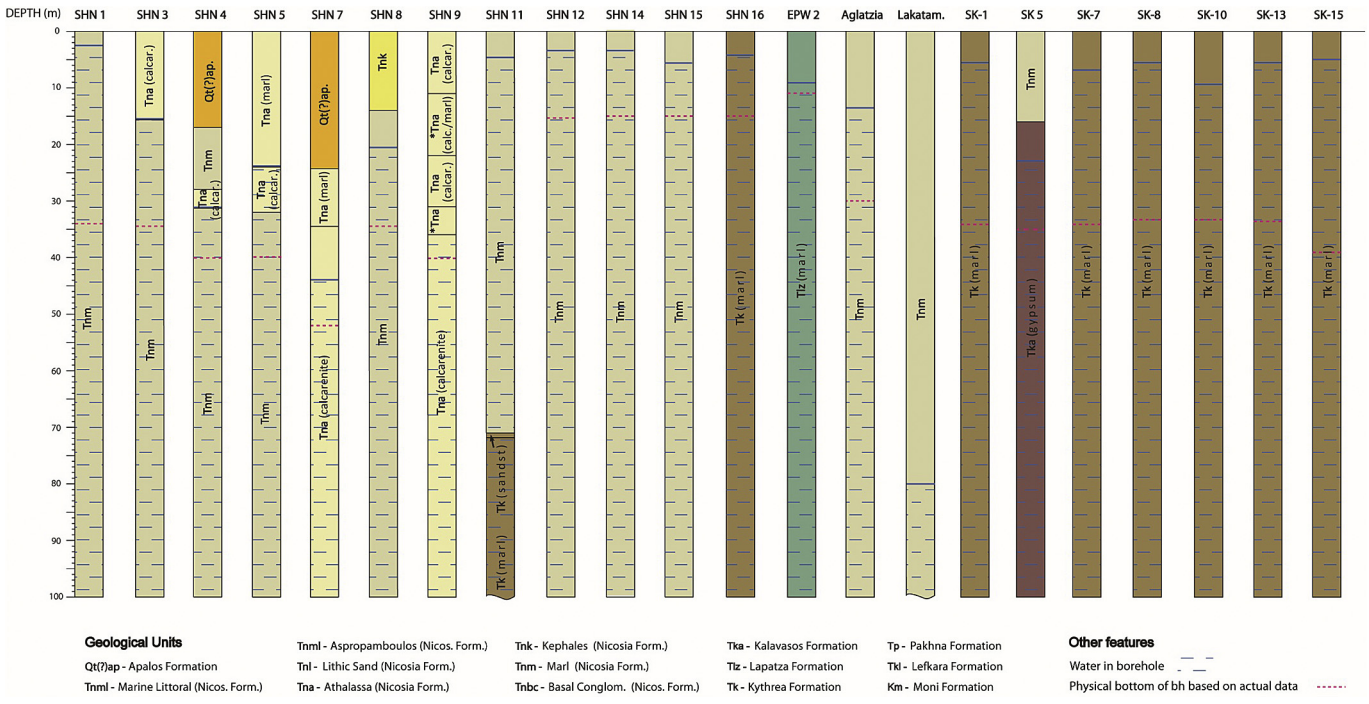

Fig 8. Geological borehole logs of the twenty-two study cases as used in FlexPDE software.

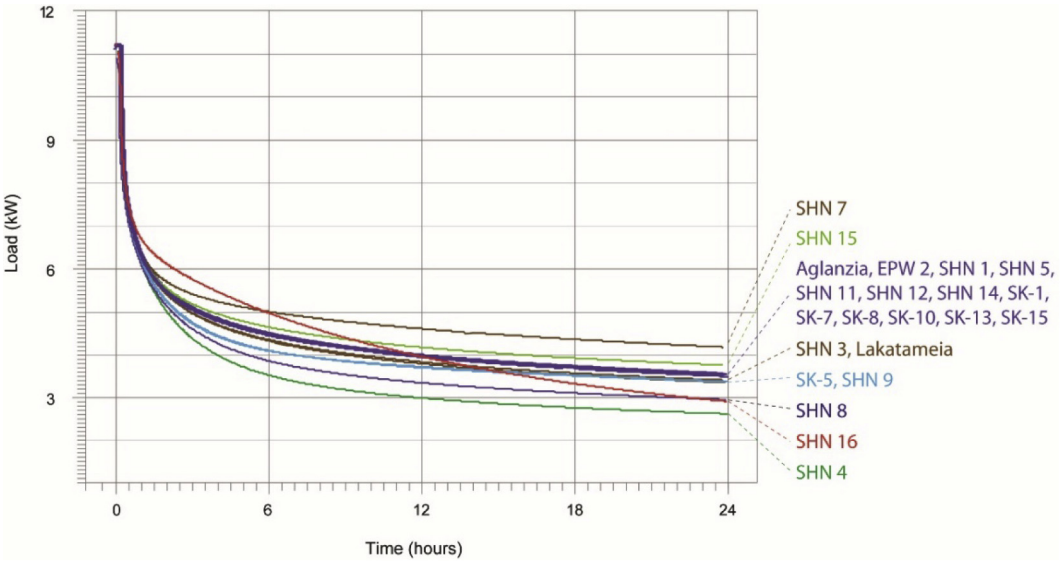

Fig 9. GHE heat loss (kW) for each study case as calculated by FlexPDE software.

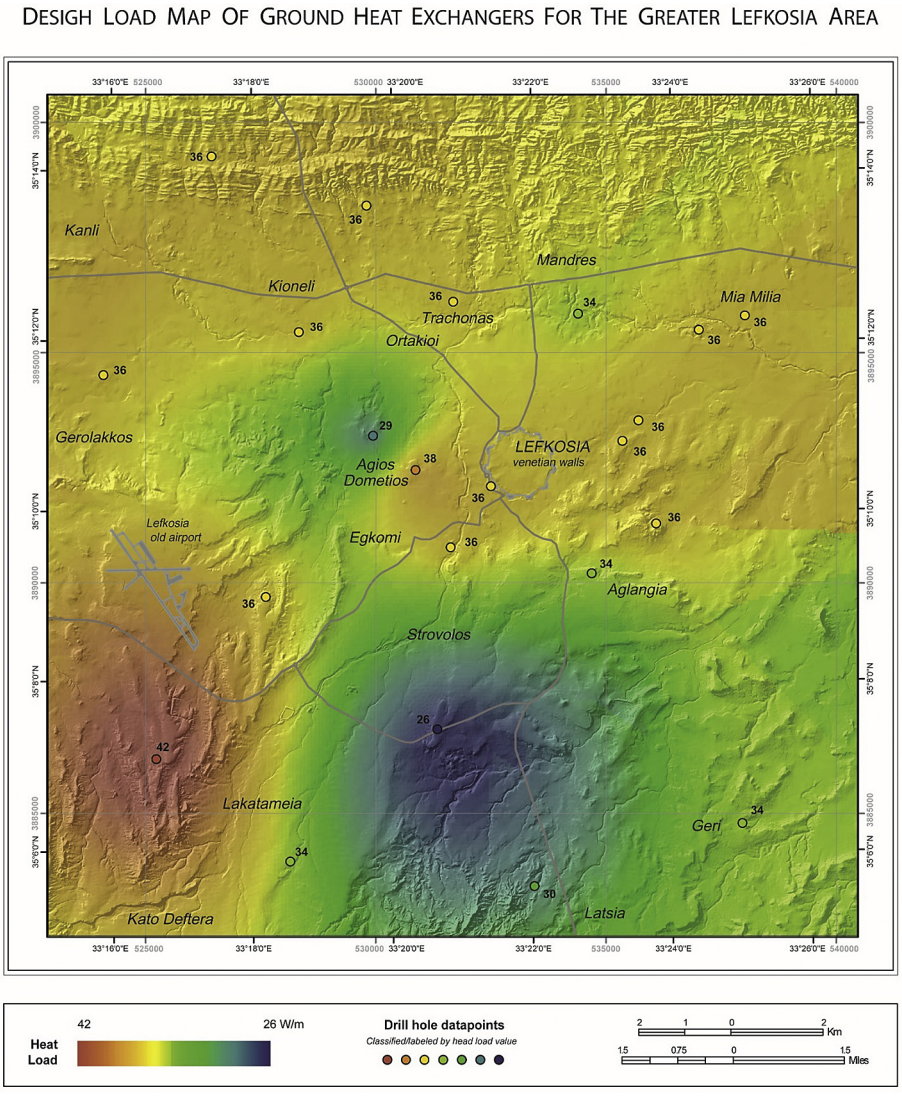

Fig 10. GHE heat loss map for the Greater Lefkosia Area (for GHEs up to 100 m depth, after 24 h of operation).

Table 4
Thermal heat exchange load of GHE from different projects.

Study Area/country	Exchange load W m^{-1} (cooling mode)	GHE type	Source of information
Lefkosia (Cyprus)	26–42	Close loop	current paper
Baden-Wurttemberg (Germany)	33–63	Close loop	[9]
Tokyo (Japan)	40–42	Close loop	[30]
Chikushi Plain (Japan)	22–31	Close loop	[21]
England & Wales	Areas are classified as favorable and less favorable for GHPS applications	Open loop	[4] [3] [2]
France	Areas are classified as favorable and less favorable for GHPS applications	Close and open loop	[7]
Ireland	Areas are classified as favorable and less favorable for GHPS applications	Close and open loop	[10]

Table 5
Thermal conductivity values (λ) from different projects.

Study Area/Country	Thermal Conductivity (W m^{-1} K^{-1})	Source of Information
Lefkosia (Cyprus)	0.6–1.5	current paper
Oslo (Norway)	1.0–6.9	[29]
Trentino (northern Italy)	0.18–4.5	[16]
Calabria (southern Italy)	0.4–3.0	[37]
Constanta (Romania)	Areas are classified as: low (<0.9 W m^{-1} K^{-1}), medium low (0.9–1.1 W m^{-1} K^{-1}), medium (1.1–1.3 W m^{-1} K^{-1}), medium high (1.3–1.5 W m^{-1} K^{-1}), and high conductivity (≥1.5 W m^{-1} K^{-1}) areas	[17]

5. Similar studies and GIS applications in other countries

The following section gives some examples of how similar approaches to evaluate the suitability of a location/area for GSHPs was applied in other studies. Most of them demonstrate a series of maps: heat flow, estimated temperatures, geological maps (geology, geotechnical properties) and underground water level maps in comparison with GHEs suitability maps.

Maximum and minimum calculated values of similar projects are presented in Table 4 below. Heat exchange load values of GHEs are in a range of 22–63 W m^{-1} and although a similar approach can be adopted in all cases for closed loop systems, the final length of the GHE varies depending on the country/area and the site-specific geology (geology, water level, porosity, etc.). All values can be used only as an indication, as underground site-specific conditions may vary in each case. The large scale web applications developed for France, Ireland, England and Wales do not take into consideration the local special underground conditions and, therefore, they classify the areas only as favorable and less favorable, without giving an actual heat exchange value.

A number of projects presenting thermal conductivity maps can also be found in international libraries. Thermal conductivity maps were also proposed as a tool for evaluating the suitability of a place for GHE installations. Thermal conductivity values illustrated in Table 5 clearly show that there is no connection between the thermal properties of rocks that are found in different countries and for each country/area separate measurements of thermal conductivity should be taken.

6. Conclusions

The current research has focused on a methodology of measuring and analyzing the thermal properties of the lithologies encountered in an area, which can then be used for the prediction of heat injection rates of a GHE in a selected area. The proposed methodology can be applied in any vertical GHE as it describes (a) the full procedure of sampling and thermal testing, (b) the compilation of thermal conductivity and thermal diffusivity maps with the use of GIS, (c) the basic formulas used for calculating the geothermal response of a vertical borehole with respect to the water lever, porosity and the thermal properties of each lithology present in the borehole, and finally (d) the compilation of a heat load map.

Regarding the area that was used as a study case, the Greater Lefkosia Area in Cyprus is an area with high potential in usage of vertical GHEs due to its geological conditions. The “Design Load Map of Ground Heat Exchangers for the Greater Lefkosia Area” was compiled in order to identify areas favorable for installation of Ground Heat Source Pumps and to provide engineers with a useful guide for sizing vertical GHEs. Values presented on the map are between 26 and 42 W m^{-1} for GHEs of up to 100 m depth, after 24 h of operation in cooling mode.

For the compilation of the map, the thermal properties of the ground were required and geological sampling for collecting and measuring samples was carried out. Recorded values are in a range of values for each thermal property of each geological formation. Thermal conductivity λ for the encountered geological formations varies from 0.5 to 1.5 W m^{-1} K^{-1}, while specific heat capacity *cp* from 0.6 to 1.0 J K^{-1} kg^{-1}. Each geological formation consists of several lithologies, characterized by different degrees of weathering and fracturing. In the same formation these lithologies locally cause variations in open porosity and, thus of the thermal properties of rocks. Values may also vary due to the different types of impurities that each sample may have. Both properties, thermal conductivity λ and specific heat capacity *cp* are presented in separate maps, which give the geographical aspect of the thermal properties in the area.

Water level was also considered in calculations, as the flow of underground water has an important effect on the cooling of the vertical heat columns of the heat exchangers. Heat load values that can be transferred to the ground through GHEs are proportionally related (a) to the level of groundwater, and (b) to the density of the underground where the borehole is located. As the level of water and the density of the soil/rock increases, heat exchange rate increases too. The only exception is the borehole where Gypsum is present, with heat loss decreasing as the water level increases.

Additionally, the heat load transferred to the earth through the GHEs in the north part of the study area is slightly higher than the amount of heat loss occurring in the southern areas. This is due to the level of water, which is higher in the north part. Also, this change of heat load values from the North to the South that can be observed on the “Design Load Map of Ground Heat Exchangers for the Greater Lefkosia Area” (Fig. 10), can also be interpreted as the boundary between the Kyrenia terrane and the Circum Troodos

Sedimentary Succession.

Upon reviewing similar studies and GIS applications referring to other countries, it turns out that the heat exchange load values of GHEs vary from 22 to 63 W m^{-1}. The magnitude of the values is a major factor for deciding the depth of the GHE. It must be stressed though that these values can only be considered as indicative, since the place site-specific conditions may vary in each case. The reviewing process has shown that there is not necessarily any connection between the thermal properties of rocks that are found in different countries, and that for each country/area a separate measurement of thermal conductivity should be performed.

Acknowledgments

This paper is dedicated to the geologist Ioannis Panayides who has inspired the compilation of this work.

References

[1] Abdulagatova Z, Abdulagatov MI, Emirov NV. Effect of temperature and pressure on the thermal conductivity of sandstone. Int. J. Rock Mech. Min. Sci. 2009;46(2009). 1055e1071.
[2] Abesser C. User Guide - Web tool for the initial assessment of subsurface conditions for open-loop ground source heat pump installations (West Midlands), British Geological Survey. 2012. Energy Science Programme, Open Report OR/12/069.
[3] Abesser C, Lewis M. The open loop ground source heat pump screening tool for England and Wales. 2013. European Geothermal Congress 2013, Pisa, Italy, 3–7 June 2013.
[4] Abesser C, Lewis MA, Marchant AP, Hulbert AG. Technical Note: mapping suitability for open-loop ground source heat pump systems: a screening tool for England and Wales, UK. Q J Eng Geol Hydrogeology 2014;47:373–80.
[5] Applied Precision. ISOMET, User manual. 1999. Bratislava.
[6] Bear J, Bachmat Y. Introduction to modeling of transport phenomena in porous media, theory and applications of transport in porous media, 4. Springer Science & Business Media; 1990.
[7] Bezelgues S, Martin J, Schomburgk S, Monnot P, Nguyen-The D, Nguyen D, et al. Geothermal potential of shallow aquifers: decision-aid tool for heat-pump installation. In: Proceedings world geothermal congress 2010, Bali, Indonesia; 2010. p. 25–9. April 2010.
[8] Bidarmaghz A, Narsilio G, Johnston I. Numerical modeling of ground heat exchangers with different ground loop configurations for direct geothermal applications. In: Proceedings of the 18th international conference of soil mechanics and geotechnical engineering, Paris. Australia: Deparment of Ifrastucture Engineering, The University of Melbourne; 2013.
[9] Blum P, Campillo G, Kölbel T. Techno-economic and spatial analysis of vertical ground source heat pump systems in Germany. Energy 2011;36(2011): 3002–11.
[10] Buckley C, Ove Arup and Partners Ltd, Ric Pasquali R, GeoServ, Monica Lee M, John Dooley J, et al. Ground source heat & shallow geothermal energy, geological survey of Ireland, homeowner manual. 2015. Version 1.0, March 2015.
[12] Busby J. UK shallow ground temperatures for ground coupled heat Exchangers. Q J Eng Geol Hydrogeology 2015. http://dx.doi.org/10.1144/qjegh2015-077. downloaded from, http://qjegh.lyellcollection.org/. at University of Toronto on December 1, 2015.
[13] Census of Population. Statistical Service of Republic of Cyprus. 2011.
[14] Christodoulides P, Florides G, Pouloupatis P, Messaritis V, Lazari L. Ground heat exchanger modeling developed for energy flows of an incompressible fluid. Word Acad Sci Eng Technol 2012;63:2012.
[15] Christodoulides P, Florides G, Pouloupatis P. A practical method for computing the thermal properties of a Ground Heat Exchanger. Renew Energy 2016;94: 81–9.
[16] Vettorato D, Geneletti D, Zambelli P. Spatial comparison of renewable energy supply and energy demand for low-carbon settlements. Cities 2011;28(2011): 557–66.
[17] Vijdea A, Weindl C, Cosac A, Asimopolos N, Bertermann D. Estimating the thermal properties of soils and soft rocks for the ground source heat pumps installation in Constanta country, Romania. Therm Anal Calorim 2014;118(2014):1135–44. http://dx.doi.org/10.1007/s10973-014-3951-8.
[18] Fabien D, Xavier P, Regis O, Antoine D. Enhancement of geothermal borehole heat exchangers performances by improvement of bentonite grouts conductivity, Vol. 33–34; 2011. p. 92–9. February 2012.
[19] Fan R, Jiang Y, Yao Y, Shiming D, Ma Z. A study on the performance of a geothermal heat exchanger under coupled heat conduction and groundwater advection. Energy 2007;32(2007):2199–209.
[20] Florides G, Theofanous E, Stylianou II, Tassou S, Christodoulides P, Zomeni Z, et al. Modeling and assessment of the efficiency of horizontal and vertical ground heat exchangers. Energy 2013;58(2013):655–63.
[21] Fujii H, Inatomi T, Itoi R, Uchida Y. Development of suitability maps for ground-coupled heat pump systems using groundwater and heat transport models. Geothermics 2007;36(2007):459–72.
[22] Fujii H, Komaniwa Y, Onishi K, Chou N. Improvement of the capacity of ground heat exchangers by water injection. GRC Trans. 2013;37.
[23] Geological Map of Cyprus. Geological survey department of Cyprus. 1995. revised, 1 map, scale 1:250000.
[24] Gorgulu K, Duruturk SY, Demirci A, Poyraz B. Influences of uniaxial stress and moisture content on the thermal conductivity of rocks. Int. J. Rock Mech. Min. Sci. 2008;45(2008). 1439e1445.
[25] Gustav B. Internal heat of the globe, Vol. I. Chemistry and Technology, University of Bonn; 1840.
[26] Harrison R, Newell W, Panayides I, Stone B, Tsiolakis E, Necdet M, et al. Bedrock geologic map of the greater Lefkosia area, Cyprus, U.S. Geological survey scientific Investigations map. 2008. 3046, 1 map, scale 1:25, 000, 36-p. text. ISBN 978-1-4113-2323-0, Pamphlet to accompany Scientific Investigations Map 3046, ISBN 978–1–4113–2323–0.
[27] Heath R. Basic ground-water hydrogeology: U.S. Geological Survey. Water-Supply Paper 2220. 1983. p. 86.
[28] Holmberg H, Acuña J, Næss E, Sønju Otto K. Deep borehole heat exchangers, application to ground source heat pump systems. In: Proceedings world geothermal congress 2015, melbourne, Australia; 2015.
[29] Ramstad KR, Midttømme K, Liebel TH, Frengstad SB, Willemoes-Wissing B. Thermal conductivity map of the Oslo region based on thermal diffusivity measurements of rock core samples. Bull Eng Geol Environ 2014. http://dx.doi.org/10.1007/s10064-014-0701-x.
[30] Nam Y, Ooka R. Development of potential map for ground and groundwater heat pump systems and the application to Tokyo. Energy Build 2011;43(2011):677–85.
[31] Neuendorf K, Mehl J, Jackson J. Glossary of geology. Fifth Edition. Alexandria, Virginia: American Geosciences Institute; 2011. Revised, ISBN 978-0-922152-89-6.
[32] Panayides I. In: Gillespie R, Glague D, editors. Encyclopedia of islands. University of California Press; 2009. p. 212–6.
[33] Pouloupatis P, Florides G, Tassou S. Measurements of ground temperatures in Cyprus for ground thermal applications. 2010.
[34] ReGeoCities Project: Developing Geothermal Heat Pumps in Smart Cities and Communities, Authors: European Geothermal Energy Council (EGEC), Belgium Universidad Politécnica de Valencia (UPVLC), Spain Romanian Geoexchange Society (RGS), Romania Bureau Recherches Géologiques Minières (BRGM), France UBeG GbR of Wetzlar (UBEG), Germany Centre for Renewable Energy Sources and Saving (CRES), Greece SP Technical Research Institute of Sweden (SP), Sweden Nationale Geologiske Undersøgelser for Danmark og Grønland (GEUS), Denmark SLR Consulting (SLR), Ireland IF Technology (IF), The Netherlands Scuola Superiore di Studi Universitari e di Perfezionamento Sant'Anna (SSSA), Italy Service Public de Wallonie (SPW), Belgium, 2015.
[35] Rybach L, Sanner B. Ground-sourcen heat pump systems – the European Experience, GHC Bulletin. 2000. March 2000.
[36] Sanner B, Karytsas C, Mendrinos D, Rybach L. Current status of ground source heat pumps and underground thermal energy storage in Europe. Geothermics 2003;32(2003):579–88.
[37] Sipio DE, Galgaro A, Destro E, Teza G, Chiesa S, Giaretta A, Manzella A. Subsurface thermal conductivity assessment in Calabria (southern Italy): a regional case study. Environ Earth Sci. 2014. http://dx.doi.org/10.1007/s12665-014-3277-7.
[38] Standard ISO 17628. Geotechnical investigation and testing – geothermal testing- Determination of thermal conductivity of soil and rock using a borehole heat exchanger. 2015.
[39] Stylianou II, Tassou S, Christodoulides P, Panayides I, Florides G. Measurement and analysis of thermal properties of rocks for the compilation of geothermal maps of Cyprus. Renew Energy 2016;88(2016):418–29.
[40] Svec JO, Goodrish EL, Palmer HL. Heat transferred Characteristics of in-ground heat exchangers, 7. Ottawa, Canada: National Research Council of Canada; 1983. p. 265–78. K1A OR6, Energy Research, 1983.
[41] Sweet J. Pressure effects on thermal conductivity and Expansion of geologic materials. Master Thesis. 1979. SAND78–1991 Unlimited Release.
[42] Tong F, Jing L, Zimmerman WR. An effective thermal conductivity mode of geological porous media for coupled thermo-hydro-mechanical systems with multiphase flow. Int J Rock Mech Min Sci 2009;46(2009):1358–69.
[43] Xenophontos C, Malpas JG. Field Excursion Guidebook, symposium Troodos 87 Ophiolites and ocean Lithosphere. 1987. p. 7–19.

Nomenclature

c_p: specific heat capacity, J kg^{-1} K^{-1}
T: temperature, °C
V: volumetric heat capacity, J m^{-3} K^{-1}
t: time, s
Q: heat source, head load, amount of heat energy, W
u: velocity, m s^{-1}
m: mass, kg

Greek symbols

λ: thermal conductivity, W m^{-1} K^{-1}
α: thermal diffusivity, m^2 s^{-1}
θ: porosity, %
ρ: density, kg m^{-3}
τ: time, s

Subscripts

w: water
eff: effective
s: soil/hard rock
f: final
i: initial